Industria: Jurnal Teknologi dan Manajemen Agroindustri
Volume 11 No 1: 51-63 (2022)

Industria: Jurnal Teknologi dan Manajemen Agroindustri
http://www.industria.ub.ac.id
ISSN 2252-7877 (Print) ISSN 2548-3582 (Online)
https://doi.org/10.21776/ub.industria.2022.011.01.6

Simple Vision System for Apple Varieties Classification

Sistem Visi Sederhana untuk Klasifikasi Jenis Buah Apel

Aulia Muhammad Taufiq Nasution[1]*, Syakir Almas Amrullah[2]
[1]Department of Engineering Physics, Faculty of Industrial Technology and System Engineering,
Institut Teknologi Sepuluh Nopember, Kampus ITS Sukolilo, Surabaya 60111, Indonesia
[2]Center for Textile, Ministry of Industry Republic of Indonesia,
Jl. Jenderal Achmad Yani No. 390, Bandung, 40272, Indonesia
*anasution@ep.its.ac.id
Received: 19th March, 2022; 1st Revision: 20th April, 2022; 2nd Revision: 27th April, 2022; Accepted: 13th May, 2022

Abstract

Every variety of apple has its particular physical characteristics, which are affected by different pre-harvest factors. Manual classification of these varieties by human labor has several weaknesses, such as the inconsistency, subjectivity, fatigue and different accuracy due to different level of experience of the inspector. This study was aimed to design and evaluate a simple computer-based vision system for recognizing and grading several varieties of apples based on their physical characteristics. Images of apples were taken and were used as training data with different algorithms to extract the particular characteristics of each variety, such as color and shape. The extracted Hue color channels and contour vector were recorded as the reference data and were used to recognize the similar characteristic of those images from the testing data group. The *k*-nearest neighbors algorithm was used to decide whether an apple belongs to a particular variety. The results show that the recognition rate based on color only was between 84–97% and it was between 5–77% it is based on the shape only. Rotating the image significantly increases the recognition rate (to be between 5 - 69% based on the shape only). Moreover, combining both color and shape characteristics significantly improves the recognition rate.
Keywords: apple's varieties classification, color signatures, combined color-morphology signatures, morphology signature, vision system

Abstrak

Setiap jenis buah apel memiliki penciri fisik spesifik, yang dipengaruhi oleh berbagai faktor pra-panen. Teknik klasifikasi manual memiliki banyak kelemahan, antara lain adalah subjektifitas, ketidakkonsistenan, kelelahan fisik dan psikologis, serta tingkat pengalaman dari petugas yang melakukannya. Tujuan studi ini adalah melakukan proses desain dan pengujian suatu sistem visi sederhana berbasis komputer untuk mengenali dan mengklasifikasi berbagai jenis buah apel berdasarkan penciri spesifiknya. Citra buah apel dari sampel latih diproses dengan berbagai algoritma untuk mengekstraksi berbagai parameter pencirinya, yaitu parameter warna dan bentuk. Informasi histogram kanal warna Hue dan vektor kontur hasil ekstraksi kemudian disimpan sebagai data referensi dan digunakan sebagai pembanding terhadap parameter serupa dari citra data uji. Keputusan diambil menggunakan algoritma K-Nearest Neighbors. Hasil menunjukkan bahwa laju pengenalan berbasis fitur tunggal warna berkisar antara 84–97%, sementara berbasis fitur tunggal morfologi berkisar antara 5–77%. Perubahan orientasi sampel sebagai data training akan meningkatkan laju pengenalan berbasis fitur tunggal morfologi secara signifikan, yaitu dari 5% menjadi 69%. Penggabungan dua fitur penciri warna dan morfologi dapat meningkatkan laju pengenalan lebih baik lagi.
***Kata Kunci**: klasifikasi jenis buah apel, penciri warna, penciri morfologi, gabungan penciri warna dan morfologi, sistem visi*

INTRODUCTION

A large amount of agricultural production and the need to classify products within specific parameters make introducing agricultural products one of the most critical stages before a sale or further processing (Behera et al., 2020). The grouping or assessing of fruit quality depends on the quality parameters used. In general, these determining parameters (Witus et al., 2018; Bhargava et al., 2021) can be divided into two major groups called internal parameters, such as

taste, aroma, acidity, sugar content, and nutritional content, and external parameters obtained from the fruit visual appearance such as size, shape, color, physical defects, and texture. Likewise, the apple type and quality can be determined based on color, shape, stalk, taste, and several other parameters. This difference in physical parameters impacted its physicochemical features (Teixeira et al., 2020), which are strongly influenced by pre-harvest management conditions (Arshad et al., 2014).

The traditional identification and sorting process using human labor has several limitations due to its subjective nature. Human perception can be misled when measuring apples' texture, color pattern, smell, and other characteristic features. In addition, the character of manual inspections, which is highly dependent on experience, training, and duration of work, as well as environmental and psychological conditions, can impact the emergence of inconsistencies and non-uniformity of results or processing time (Bhargava & Bansal, 2021).

Generally, a computer vision-based inspection system consists of two main components: a camera as a sensor for data acquisition and a data processing system. This system has been implemented for various analytical uses of food and agricultural products, such as bakery products (Goñi et al., 2017; Nashat et al., 2016), meat (Taheri-Garavandet al., 2019), and fish (Mathiassen et al., 2012), vegetables and fruits (Tripathi et al., 2020; Bhargava et al., 2021; Bhargava et al., 2022), wheat (Laabassi et al., 2021), as well as applications in various other fields such as medical diagnostics (Khanam et al., 2019), automation (Tian et al., 2020), remote sensing (Song et al., 2019), and forensics (Bedeliet al., 2018).

The use of computer vision technology in agriculture is generally based on two goals: quality assessment (Bhargava & Bansal, 2021) and product defect search (He et al., 2021). Computer vision technology has also performed tasks such as shape classification, product defect detection, and product variety classification. Because of its fast, economical, consistent, and objective properties, this technique has begun to be widely used for inspection and evaluation purposes, so it can be used as an alternative to avoid errors that arise in the manual inspection process in determining apple varieties (Li et al., 2021).

As the biggest tropical country in Southeast Asia, Indonesia has a wide variety of fruit trees, i.e., around 300 different types of indigenous fruit, and about 270 species have been identified as edible fruits (Uji, 2007). Several types of these fruits are nearly identical in color, texture, or even shape by nature, making them difficult to distinguish from one another. Advancements in computer vision technology offer a benefit that can be implemented to solve these tasks. Simple vision systems that can be easily adapted to recognize and grade indigenous Indonesian fruits would benefit this context. Additionally, the ease and speed of accomplishing such grading and sorting tasks are beneficial in reducing time and labor costs, which will eventually increase the values of sold products, which also means better income for the farmers.

In this study, efforts were described to develop a simple and low-cost vision system by incorporating necessary algorithms to extract essential features that recognize and discriminate apple varieties based on their morphological and color characteristics. The work began with designing a low-cost webcam-based image acquisition system with a uniform LED lighting system. This uniform lighting system was thought to be a key factor in reducing glare from reflected light from the apple's skin, which could affect the subsequent recognition stage. The developed system was then trained to recognize the necessary features for distinguishing and recognizing apple fruit variants. This study used three apple varieties: Anna, Fuji, and Red-Delicious. In order to improve the performance of the developed system, factors that influence recognition rates were investigated.

METHODS

Several stages in the development process will be explained in this section, as well as the required testing to assess the performance of the developed system.

Lighting System and Image Acquisition

A computer vision system generally consists of five essential components: lighting systems, cameras, frame grabbers or digitizers, computer hardware, and software. The experimental setup used for acquiring apple images can be depicted in Figure 1.

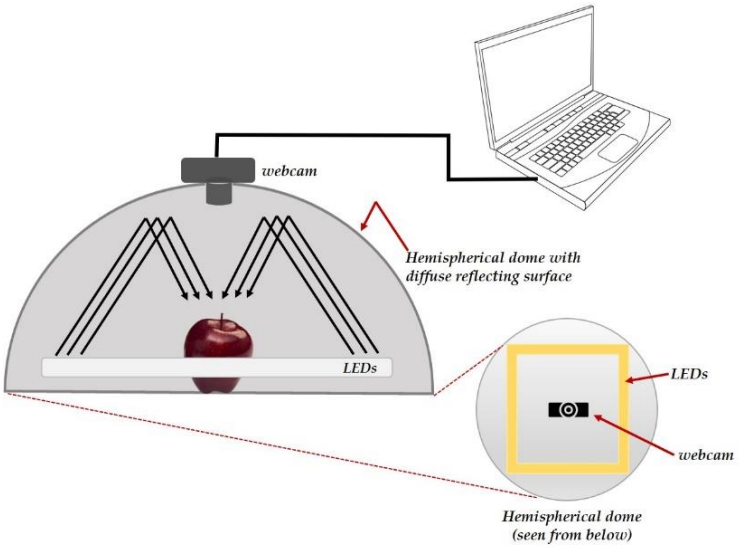

Figure 1. Experimental Setup used During this Reported Study

This study used a Logitech C170 CCD camera with a 5-megapixel resolution and produced an image the size of 640x480 pixels. The light was generated by a linear array of LED chips arranged in a rectangular shape and faced a hemispherical dome. The hemispherical dome, with a diameter of 35 cm, was made using a plastic food cover coated with fabrics glued onto its walls and painted with silver spray paint to produce a diffusely reflecting surface on its inside walls. The diffusely reflected light from LEDs lighted up the samples, passed through the camera lens, and projected onto the sensor surface, acquired, converted, and eventually stored in a digital format. The process of converting images into numeric form is also known as digitization. The image was mapped into two-dimensional coordinates where each point consists of one pixel using a frame grabber (Brosnan & Sun, 2004). The digitization process was carried out in the electronics system inside the camera components and transferred via a USB interface in real-time using dedicated computer software.

Extraction of Visual-related Features

Digital images can be used to obtain physical information from objects recorded on an image. Each type of object has characteristics that distinguish it from other objects. If it is traced back from behind, then the extraction of specific information in an image can be used to explain or recognize the types of objects in the image. In this research, the identification of apple varieties was made by extracting physical information in the form of color and the object's geometry from its two-dimensional acquired image. At this stage, the visual signatures of the object were quantified as the object's characteristics, which were used for comparison purposes in the next stage. The explanation related to the mathematical basics used computationally for extraction and recognition were explained in these subsequent sub-sections.

Segmentation of Acquired Apple Images

One of the most fundamental problems in digital image processing is image segmentation. In image analysis, image segmentation is also a necessary step. Image segmentation is partitioning a digital image into multiple segments in digital image processing and computer vision (sets of pixels, also known as "super pixels"). Segmentation is breaking down an image into its constituent parts or objects. Segmentation aims to make an image more meaningful and easier to analyze by simplifying and/or changing its representation. Image segmentation is a technique for locating objects and boundaries in images (lines, curves, edges, and others). In more technical terms, image segmentation assigns a label to each pixel in an image so that pixels with the same label have similar visual characteristics. A digital image (made up of pixels or picture elements) is mathematically defined as a two-dimensional function $f(x, y)$,, with x and y being spatial (plane) coordinates. The intensity "or" grey level of the image at any pair of coordinates (x, y) is the value of "f" at that point. In the case of

digital image processing, various image segmentation techniques are used (Chaudhary & Yogesh, 2019).

Edge detection techniques are one of the most natural techniques for image segmentation. An image's edge is one of its most basic features. For image segmentation, edge detection can be used as a primary tool. The image edges contain a significant amount of information critical for obtaining the image characteristic through image analysis. In a grayscale image, the edge is a local feature that divides two regions, each of which has a grey level that is more or less uniform, with different values on the two sides of the edge, within a neighborhood. Several edge-detection algorithms can be implemented for edge-detection (Mutneja, 2015). In this reported work, a Canny edge detection algorithm was implemented to segment the fruit's outer edge from its surroundings.

Extraction of Morphological Features

In image processing, the concept of the moment helps identify an object's characteristics in an image. Meanwhile, the concept of "moment" is closely related to probability theories in statistics. A probability function, for example, can be written as *p (x)*, which represents a distribution of variable x; thus, the *n-th* moment of this function can be written as equation 1 (Solomon & Breckon, 2011).

$$m_n = \int_{\infty}^{\infty} x^n p(x) dx \qquad (1)$$

If *n* is zero-value (the zeroth moment), then the function provides an area under the curve of $p(x)$. Meanwhile for the first moment, i.e., for *n=1*, it is the mean from the x variables. Central moment from the density function which represents the variation of the mean can be defined using equation 2 (Solomon & Breckon, 2011).

$$M_n = \int_{\infty}^{\infty} (x-\mu)^n p(x) dx \qquad (2)$$

M_n is the *n-th* central moment, x is the random variables, μ is the mean, and the $p(x)$ is the density function. Meanwhile, higher-order moment, i.e., with *n > 2,* provides information regarding the form of the density function. The recognition of the unique values of all moments gives a distinctive feature of the density function, where the value of each of these moments simultaneously stores the shape information of the density function.

Calculating the moment value in the image is performed by placing the image intensity function *I(x,y)* instead of the *p(x)* function. Calculating this moment value describes the characteristics of the shapes in the image. Hu was firstly offered in 1962 with two-dimensional moment invariant theory for 2D images, where there are seven-moment equations invariant to translation, rotation, or scaling operations (Ouchtati et al., 2019). It consists of six absolute orthogonal invariant moments, i.e., second and third-order moments as given in equation 3, and one orthogonal invariant skew moment equation as given in equation 4 (Hu, 1962).

The notation of μ_{ij} refers to the normalized central moment of 2-dimensional area, i.e. with the i^{th} is for the first dimension and the j^{th} is for the second dimension. The shape feature extraction process begins with detecting the edges in the image. The Canny edge detection algorithm is used at this stage (Sekehravani et al., 2020). The results of Canny edge detection are limited only to the determination of edges and the negation of pixels outside the edges. However, they do not provide numerical information regarding the object's shape in the image, so the next step is to read the image contours.

$$momen\ 1 = \mu_{20} + \mu_{02}$$
$$momen\ 2 = (\mu_{20} - \mu_{02})^2 + 4\mu^2{}_{11}$$
$$momen\ 3 = (\mu_{30} - 3\mu_{12})^2 + (3\mu_{21} - \mu_{03})^2$$
$$momen\ 4 = (\mu_{30} + 3\mu_{12})^2 + (3\mu_{21} + \mu_{03})^2$$
$$momen\ 5 = (\mu_{30} - 3\mu_{12})(3\mu_{30} + \mu_{12})[(\mu_{30} + \mu_{12})^2 - 3(\mu_{21} + \mu_{03})^2] + (3\mu_{21} - \mu_{03})(\mu_{21} + \mu_{03})[3(\mu_{30} + \mu_{12})^2 - (\mu_{21} + \mu_{03})^2]$$
$$momen\ 6 = (\mu_{20} - \mu_{02})[(\mu_{30} + \mu_{12})^2 - (\mu_{21} + \mu_{03})^2] + 4\mu_{11}(\mu_{30} + \mu_{12})(\mu_{21} + \mu_{03}) \qquad (3)$$
$$momen\ 7 = (3\mu_{21} - \mu_{03})(\mu_{30} + \mu_{12})[(\mu_{30} + \mu_{12})^2 - 3(\mu_{21} - \mu_{03})^2] - (\mu_{30} - 3\mu_{12})(\mu_{21} + \mu_{03})[3(\mu_{30} + \mu_{12})^2 - (\mu_{21} - \mu_{03})^2] \qquad (4)$$

Contours are several points that represent shapes or curves that exist in the image. Contour information is represented in vector quantities that provide information on the distribution of points in the image. This point vector then forms a closed contour to be used in calculating the Hu moment (Liu et al., 2019a). The visual characteristics of the object are then being quantified to later become the object's characteristics for the comparison process at the next stage.

Extraction of Color Features

Testing the Hue saturation value (HSV) color space channels provides an advantage over the red green blue (RGB) space, with high consistency results from the color image of the Hue color channel even though there are differences in lighting conditions (Ajmal et al., 2018). The HSV color space can be used in the color-based object segmentation process (Nixon & Aguado, 2012).

The initial stage of the color feature extraction process is performed by transforming the RGB color space image into the HSV color space. The HSV (perceptual color) color space is more appropriate and closely resembles human perception of color than the RGB (true color) color space. The Hue color channel from the HSV color space was taken as a color marker which was analyzed further. The HSV spatial image is then broken down into its components to get a stand-alone Hue value, which was used in the comparison process in the next stage.

Mathematically, the Hue color channel value is obtained from the RGB image using the equation 5. The Hue value represents the dominant color of the image pixels. As seen in equation 5, the Hue value of the RGB image is determined by the lowest value and the highest value of each channel in the RGB space.

System Training and Knowledge-Base Building

The training process was performed to extract the apple varieties' morphological and color features. Equations 3 - 4 and 5 were used to extract these morphological and color features. Ten (10) samples of apples, each from the Anna, Fuji, and Red-Delicious varieties, were used, and all the apples were bought from the nearby supermarket. All three apple varieties tended to be red and have different fruit shapes. The use of this small number of samples was merely to demonstrate in the study how the dependency of the system's recognition rate can be improved by incorporating combinations with other essential features from the apple's fruits. The use of a larger number of samples should have been beneficial to improve the prediction models for the recognition rate (Xu & Goodacre, 2018). Hue color identifiers with histogram values and shape identifiers are taken from the vector of the image's outermost edge and then stored. The histogram values of these 30 pieces are stored as a "knowledge base," which was used as a reference in the testing process.

System Testing

The testing process was performed on 100 total samples, around 30 - 40 apples of each variety: 31 pieces for Anna varieties, 30 pieces for Fuji varieties, and 39 pieces for Red-Delicious. The test results were compared for each variety. In addition, recognition with each signature is also included to compare the resulting recognition rate.

Calculation of Shape Conformity

The shape similarity of the two images is determined by comparing the seven Hu moments given in equations 3 - 4. A Moment is a general contour characteristic calculated from the total pixels of the contour. The seven Hu moments were

$$Hue_{color\ channels} = \begin{cases} 60(G-B)/(V-min(R,G,B)\ if\ \ max(R,G,B)=R \\ 120+60(B-R)/(V-min(R,G,B))\ if\ \ max(R,G,B)=G \\ 240+60(R-G)/(V-min(R,G,B))\ if\ \ max(R,G,B)=B \end{cases} \quad (5)$$

$$\begin{aligned} I_1(A,B) &= \sum_{i=1}^{7}\left|\frac{1}{m_i^A}-\frac{1}{m_i^B}\right| \\ m_i^A &= sign(h_i^A)\cdot log\left|h_i^A\right| \\ m_i^B &= sign(h_i^B)\cdot log\left|h_i^B\right| \\ h_i^A &= Hu\ moment\_A \\ h_i^B &= Hu\ moment\_B \end{aligned} \quad (6)$$

obtained from contour information in the form of a collection of extracted point vectors. At this stage, only the most significant contours were included in the calculation. It is assumed that the image's largest contour comes from the fruit's outer surface. The method of calculating the suitability of the shape in this experiment uses the equation 6.

The degree of similarity I_1 *(A, B)* between the two forms A and B being compared was obtained from the total difference of h_i^A and h_i^B, i.e., which represent the *i-th* of each respected seven Hu moments of the two forms A and B being compared (equation 3-4). The higher the similarity between two forms, the closer the total value of the calculation to zero.

Histogram Similarity Calculation

Hue color channel histograms from test images and training or reference images were compared using the correlation method with the equation 7:

$$d(H_1, H_2) = \frac{\sum_1 H_1'(i) \cdot H_2'(i)}{\sqrt{\sum_1 H_1'^2(i) \cdot H_2'^2(i)}}$$

with

$$H_k'(i) = H_k(i) - (1/N)\left(\sum_j H_k'(j)\right) \quad (7)$$

where $H_1'(i)$ and $H_2'(i)$ represent the *i-th* bin's values of the two histogram 1 and 2 being compared, and *N* represents the number of histogram bins.

The calculation of histogram similarity requires that the number of bins is the same so that the two histograms of the Hue color channel being compared must both consist of 180 bins representing a 360-degree range of Hue values. Each bin value is according to the occurrences number of all image pixels. H_1 and H_2 refer to the two histograms being compared. Each bin of the H_1 histogram has a calculated difference with the value of the same bin of the H_2 histogram using equation (7), such as the last bin. The calculation results of this method showed that the more similar the two histograms, the greater the value is given, and vice versa. A perfect match is represented by a value of 1.

Decision-Making Algorithm

In general, building an automated classification system requires manual design and training in two aspects, namely task specification and class labeling. Task specifications determine the types of classes to be built and the parameters to be observed. The class labeling process is related to the training process (training) manually with human intervention in the initial process to build a definition recorded in the automation system (Nixon & Aguado, 2012).

One of the most common classification techniques is the K-Nearest Neighbors algorithm, commonly abbreviated as K-NN (Liu et al., 2019b). This technique first stores all the training data in the database. Furthermore, the new data to be tested is compared with all existing training data to determine the number of K (K refers to integers) at which points are closest to the test sample. The conclusion of the classification is taken by voting from several K data points, which class is repeated the most.

The decision-making process in this program design uses the basic concept of the K-Nearest Neighbor classification algorithm. The test inputs that have obtained color and shape markers were then compared with 30 color markers and 30 shape markers in the training data with the method mentioned in the previous point. The comparison results with the 30 training data sets were then sorted based on their similarity. As mentioned in the previous section, there is a difference in ordering between shape and color markers in this case. If the color identifier of the training data is more similar to the test data, the value gets closer to 1, so the values were sorted from largest to smallest. While the shape identifiers were more similar if the comparison value was closer to zero, the values were sorted from small to large. These two data sequences were then selected based on the sorted rank. Since these reference data contained identities of their varieties, only the top 5 ranked values from the color identifiers, and the top 4 ranked values from the shape identifiers were included. The choice was taken to get optimum computational efforts to extract idiosyncratic behaviors learned previously from the training set, as also recommended in Larose et al. (2014).

Furthermore, these nine top data points were as a preliminary training process, 10 samples of apples, each from the Anna, Fuji, and Red-Delicious varieties, were used, and all apples were bought from the nearby supermarket. All three apple varieties tend to be red and have different fruit shapes. The decision to use this small number

of samples was mere to demonstrate how the dependency of the system's recognition rate can be improved by incorporating combinations with other essential features from the apple's fruits. The use of a more significant number of samples should have been beneficial to improve the prediction models for the recognition rate. Hue color identifiers with histogram values and shape identifiers are taken from the vector of the image's outermost edge and then stored. The histogram values of these 30 pieces are stored as a "knowledge base," which was used as a reference in the testing process, grouped based on their varieties. Type decisions were taken by the group with the most significant members.

RESULTS AND DISCUSSION

Image Acquisition

The acquired image has several contour groups, or what is known as a hierarchy. In this study, only the outer contour of the fruit was observed for the segmentation and characterization processes. At this stage, only the largest contour was taken as a representation of the object contour, which is then used in the veiling process for image segmentation. Figure 2 shows a comparison of the acquired image and its segmentation results.

Visual Signatures Extraction

Morphological Signatures Extraction

The edge of the image that has been detected by the Canny method does not yet contain numerical information that can be used as a marker. Therefore, at this stage, the contour reading process is carried out. Contours are many points that represent shapes or curves in the image. Contour information is represented in vector quantities that provide information on the distribution of points in the image. This point vector then forms a closed contour to be used in calculating the Hu moment.

Color Signatures Extraction

The object image that has been segmented is used in the extraction process for color markers. The segmented RGB image is converted into the HSV color space. In this study, only the Hue color channel was used as a color marker, so the three-color channels in the HSV space were separated. The Hue channel histogram of the HSV image of the object is then calculated as a color marker of the observed object. Figure 3 shows the image of the object in the HSV space and the Hue channel.

An example of a histogram comparison of the three types of apples can be seen in Figure 4; with the dominant color of red, the three varieties have different histogram tendencies.

(a) (b)

Figure 2. (a) Apple Image Acquired, and (b) Apple Image After Segmentation

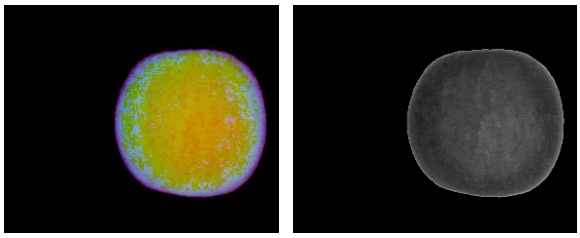

(a) (b)

Figure 3. Image of HSV Color Space (a) and Hue Color Channel (b)

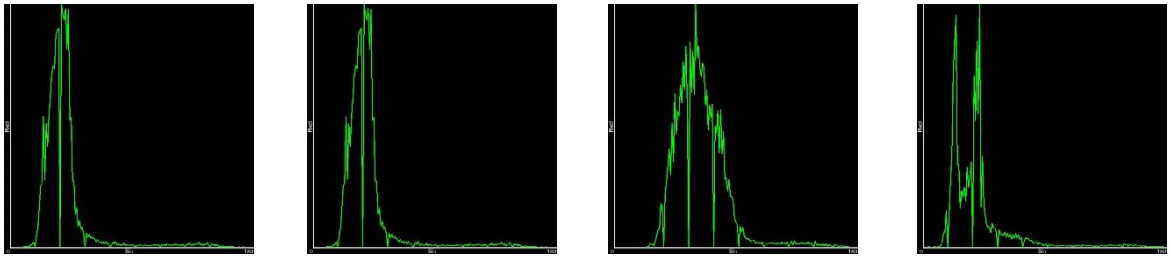

(a) Training Data from Anna Variety (b) Testing Data from Anna Variety (c) Testing Data from Fuji Variety (d) Testing Data from Red-Delicious Variety

Figure 4. Comparison of Histograms of Training Data and Test Data for Several Apple Varieties

The Anna variety sample has a peak in the 40th region, the Fuji histogram has a peak in the 50th region, and the Red Delicious variety sample histogram has two peaks in the 20th and 40th regions. These histogram values were compared with each other to determine the level of color similarity of the sample object to be recognized.

System Training and Knowledge-Base Building & System Testing

The training process is carried out in the early stages of system design to form a definition and provide a reference in the system before it is used in testing. The largest contour vector, which represents the outermost contour of the fruit that has been obtained in the preprocessing process, is reused to characterize the shape of the observed object. While the color markers are taken from the histogram matrix of the Hue color channel image, at this training stage, 10 samples from each variety were used up to the extraction stage for shape and color markers. The numerical values of these two identifiers (contour vector and histogram matrix) are stored in (.yml) format with user-defined labeling. In subsequent processes, each new test was compared with the stored value, and the system will interpret it based on the stored training data.

System testing was carried out on 100 test samples from the three varieties since some of the collected samples were considered inappropriate to be included in the testing. Of course, the use of large datasets would be beneficial to extract complete descriptions for the developed prediction model. However, it brings a consequence of the increased cost of computational complexity. Meanwhile, the use of undersized samples results in fast and efficient computation. For the experimental and comparative studies, as the case in this reported study, the choice of the small number of the sample, which provides a classifier with the higher predictive accuracy, is considered to provide the better performance (Lutu & Engelbrecht, 2006). The testing stage was a comparison of the Hue color channels histogram, calculation of shape conformity, and decision making.

Comparison of the Hue Color Channels Histogram

The higher the similarity between the training and the testing data histogram, the closer the comparison to the value 1 (Bradski & Kaehler, 2008). In Figure 4, the histogram (b), derived from the Anna varieties image, showed the highest similarity to the histogram (a), and hence it provided the highest value. When compared to the histograms (c) of the Fuji variety and the histogram (d) of the Red-Delicious variety, the histogram (c) showed a more remarkable similarity to Anna's variety histogram (b). This result is understandable because of the fruit color similarity of the red variety to the Anna variety. However, it is still less similar to the other Anna varieties (b).

Calculation of Shape Conformity

The calculation of the conformity of the shape is done by comparing the contour of the test image with the reference contour that has been saved in the steps previously mentioned. In this section, the contour information is used to calculate the contour moment, which is the characteristic obtained from the integration process of a number of pixels contained in the contour series. In this study, the contour characterization process used the seven Hue moments, in which the values of the seven Hue moments extracted from the two images were compared, and then the total difference was calculated. If the difference between the two is getting closer to zero, it indicates the shape of the two contours is getting closer (Bradski & Kaehler, 2008). As an example of this calculation, Figure 5 show the suitability calculation of same fruit shape.

In the program, the suitability calculation of shape in Figures 5b, 5c, and 5d of each of the image contours (Figure 5a) as test data using equation (6) produces a sequential value of 1.462e-02 for the Figure 5b, 1.187e-02 for the Figure 5c, and 7.914e-02 for the Figure 5d.

The higher the similarity between the contours and the Figure 5a, the value shown was closer to zero. In the example, it can be seen that among the three images, Figure 5d, which is derived from the Red-Delicious variety, has the most significant value, meaning that it has the lowest suitability. In this example, Figure 5c from the Fuji variety has a smaller suitability value than Figure 5b from the same variety as Figure 5a, indicating that using one reference provided a greater chance of wrong recognition. As previously cited (Lutu & Engelbrecht, 2006), the reference image used in this study was 30, so the comparison process is expected to have a smaller chance of recognition error.

(a) Training Data from Anna Variety

(b) Testing Data from Anna Variety

(c) Testing Data from Fuji Variety

(d) Testing Data from Red-Delicious Variety

Figure 5. Images Used for Calculation of Shape Conformity

Decision Making

In this study, the same test was performed on 100 samples; 31 Anna varieties, 30 Fuji varieties, and 39 Red-Delicious varieties. The reason for the different numbers of apples used for each variety was practical. At that time, it was realized that some of the bought apples started to rot, which was considered inappropriate to be included; eventually, they were removed from the testing. Hue color markers and shapes were extracted using the same algorithm as the reference data and compared with the Hue color markers and contour vectors from the previously-stored reference data. The recognition results comparison of the two markers can be seen in Table 1, Table 2, and the combination of the two in Table 3.

Table 1 shows the recognition results if only the color identifier is used. At 97%, the recognition rate of Red-Delicious varieties is the highest compared to other varieties in this section. This result indicates that the Red-Delicious variety is significantly different in color or has a narrower color uniformity than the other varieties and bears little resemblance to the Anna variety. The Fuji variety recognition rate is 93%, which can be understood from the distinctive color and tends to be lighter than the Anna and Red-Delicious varieties. While the Anna variety recognition rate was the lowest, five samples were recognized as Red-Delicious. This result was due to the tendency of the Anna variety to resemble Red-Delicious with its dark red color.

Table 2 shows the system recognition result if only the shape identifier is used. The recognition rate of the Red-Delicious variety is much lower than other varieties, with a percentage of 5%. Many apple shape variations might contribute to this Red-Delicious variety's lower recognition rate than other varieties used in the study. The data result supports this indication, showing that the Red-Delicious varieties' misinterpretation to be the Anna and the Fuji varieties were relatively high, 30.8% and 59%, respectively. The Anna and Fuji varieties' recognition rate was 52% and 77%, respectively. Most of the Fuji variety's misinterpretations occurred because the Anna variety confused the system. On the other hand, most of the misinterpretation of the Anna variety was caused by misinterpreting the Fuji variety. This result can be understood because there is a tendency for the two varieties to have a similar shape, so recognizing these two varieties provides errors in some samples.

Table 1. Recognition results using color signatures

Sample	Recognition Using Color Signatures					Recognition rate (%)
	Numbers	Red Delicious	Fuji	Anna	Unrecognized	
Red Delicious	39	38	0	1	0	97
Fuji	30	2	28	0	0	93
Anna	31	5	0	26	0	84

Table 2. Recognition results using morphological signatures

Sample	Recognition Using Morphological Signatures					Recognition Rate (%)
	Numbers	Red Delicious	Fuji	Anna	Unrecognized	
Red Delicious	39	2	12	23	2	5
Fuji	30	0	23	5	2	77
Anna	31	2	7	16	6	52

Table 3. Recognition results using combination of two signatures

Sample	Recognition Using Combination of Two Signatures					Recognition Rate (%)
	Numbers	Red Delicious	Fuji	Anna	Unrecognized	
Red Delicious	39	36	0	2	1	92
Fuji	30	0	28	2	0	93
Anna	31	3	0	27	1	87

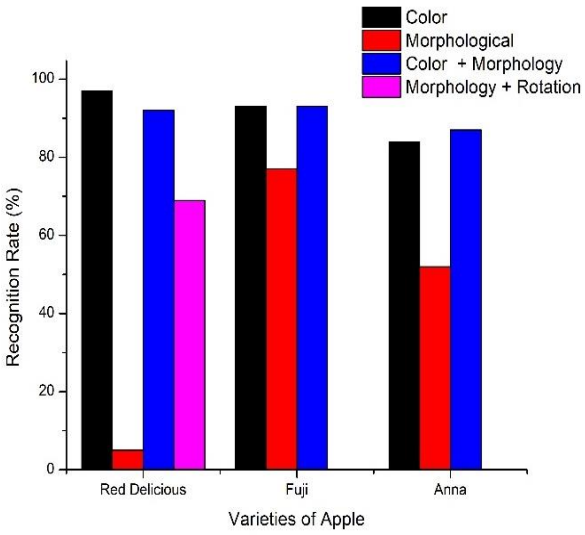

Figure 6. Comparison of Recognition Rate Based on Signature Used

The recognition results when using a color and shape signatures combination are shown in Table 3. Recognition using a combination gives better results than a single shape signature, as shown in Table 2. Compared to the results of using a single-color signature (shown in Table 1), there was a decrease in the recognition percentage of the Red-Delicious variety and an increase in the Anna varieties. Meanwhile, the recognition rate for Fuji varieties is relatively unchanged: four pieces from the Anna variety, two pieces from the Fuji variety, and three pieces from the Red-Delicious variety, which are not correctly identified. Three Red-Delicious varieties and two Fuji varieties are misinterpreted as Anna varieties, and the four Anna varieties are misread as Red-Delicious. Among the three varieties, the Fuji variety is relatively easy to recognize because the shape variants are not too different, and the color has a slightly distinctive yellow-tinged color compared to the other two types. The Red-Delicious variety does not have yellow-tinged color and is predominantly black and red but has a relatively more varied fruit shape, like the Anna variety. Although it has yellow-tinged color, some varieties of Anna have a deep red color that is sometimes confused with Red-Delicious.

The recognition rate comparison of each variety based on the signature used is shown in Figure 6. The recognition rate with a single-color identifier gave the highest result on the Red-Delicious variety compared to a single shape identifier or a combination of colors and shapes. Meanwhile, for the case of Anna and Fuji varieties, the recognition rates are higher as the combination of color and shape signatures was used. Using single shape signatures generally gives the lowest results in the performed tests. Therefore, another test was performed to examine whether the morphological features training data augmentation might enhance the system recognition. Several published works (Mikolajczyk & Grochowski, 2018; Nanni et al., 2021) have indicated that the training process data augmentation might enhance some image recognition problems. One of the possible ways to augment the training data are using rotation variations.

The training data rearrangement for the variety with the lowest percentage (Red-Delicious) is performed in this section to examine the rotation treatment effect of the reference data on the system's ability to recognize the Red-Delicious variety. So, ten training data Red-Delicious varieties were replaced with four times larger training data; 40 training data were taken from 5 Red-Delicious varieties. Each fruit was rotated in multiples of 45° (0°, 45°, 90°, 135°, 180°, 225°, 270°, 315°), so each fruit produced

eight different images, as shown in Figure 7.

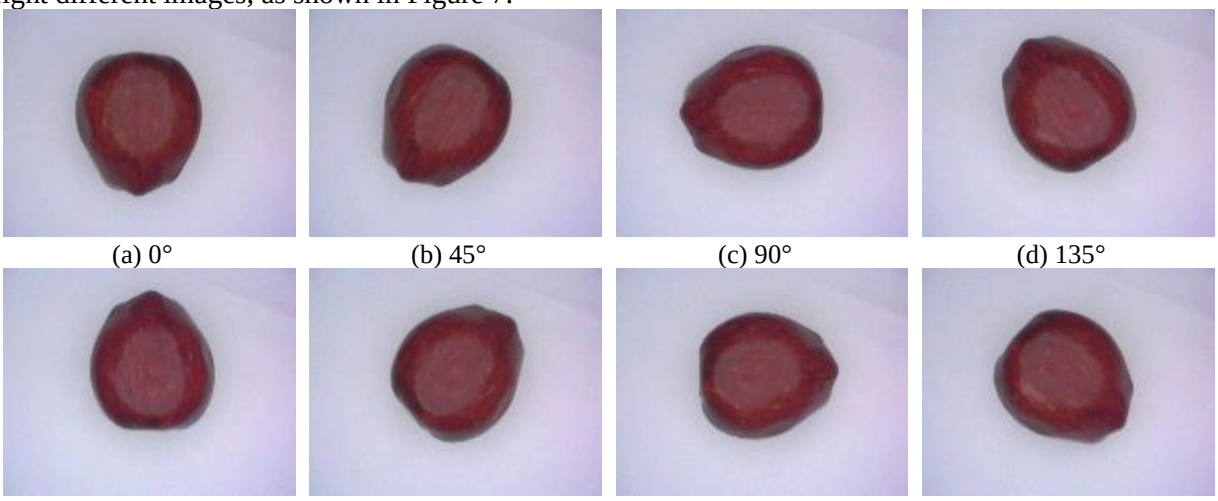

(a) 0° (b) 45° (c) 90° (d) 135°

(e) 180° (f) 225° (g) 270° (h) 315°

Figure 7. Rotation Variation in Training Data for Red-Delicious Variety

Tabel 4. Effect of rotation variation in training data to the recognition rate of Red-Delicious variety

Training Data Status	Number of Samples	Red Delicious	Fuji	Anna	Unrecognized	Recognition Rate (%)
Before rotation varied	39	2	12	23	2	5%
After rotation varied	39	27	3	9	0	69%

The five Red Delicious samples at eight different orientations were chosen solely based on the trade-off between sufficient additional reference for the recognition program and the computational time required.

Furthermore, retesting was performed on the Red-Delicious variety using the same 39 samples mentioned in Tables 1-3 and comparing the results with the previous testing using a single shape signature. From these tests, the results are shown in Table 4. Table 4 shows an increase in the recognition level of the Red-Delicious variety with variations in the training data rotation, from 5% before being given the rotational variation treatment to 69% after the training data was varied; hence there was an increase of 65% recognition rate. The fallacy of introducing Red-Delicious varieties as Anna and Fuji varieties is reduced. These results indicate a significant increase in recognition rate when the training data contains more possible angles of view of fruit images acquired.

CONCLUSIONS

The recognition rate of Red-Delicious and Fuji varieties was the best when they were identified using color feature, at 97% and 93% respectively. The recognition rate of Anna variety was around 84%. Since there are wide variation of the Red-Delicious apples shape, the level of recognition rate using only single shape feature was low, i.e., only 5%. This low recognition rate can be significantly boosted by varying fruit rotation during the training process, i.e., as a way to augment the training data. These variation in 8 rotation angles (step size of 40°) provided a significant increase in the recognition rate from 5% to 69%. Combining two features as classifiers would, in general, increase the recognition rate. Based on these results, the more the samples used in the training process, the higher the recognition rate resulted by the system.

References

Ajmal, A., Hollitt, C., Frean, M., & Al-Sahaf, H. (2018). A comparison of RGB and HSV colour spaces for visual attention models. *2018 International Conference on Image and Vision Computing New Zealand (IVCNZ), 2018-Novem*, 1–6. IEEE. https://doi.org/10.1109/ IVCNZ.2018.8634752

Arshad, M., Shahnawaz, M., Shahkeela, S., Hussain, M., Ahmad, M., & Khan, S. S. (2014). Significance of physical properties of apple fruit influenced by preharvest orchard management factors. *European Journal of Experimental Biology*, *4*(5), 82–89.

Bedeli, M., Geradts, Z., & van Eijk, E. (2018). Clothing

identification via deep learning: forensic applications. *Forensic Sciences Research*, *3*(3), 219–229. https://doi.org/10.1080/20961790.2018.1526251

Behera, S. K., Rath, A. K., Mahapatra, A., & Sethy, P. K. (2020). Identification, classification & grading of fruits using machine learning & computer intelligence: a review. *Journal of Ambient Intelligence and Humanized Computing*, (March). https://doi.org/10.1007/s12652-020-01865-8

Bhargava, A., & Bansal, A. (2021). Fruits and vegetables quality evaluation using computer vision: A review. *Journal of King Saud University - Computer and Information Sciences*, *33*(3), 243–257. https://doi.org/10.1016/j.jksuci.2018.06.002

Bhargava, A., Bansal, A., & Goyal, V. (2022). Machine learning–based detection and sorting of multiple vegetables and fruits. *Food Analytical Methods*, *15*(1), 228–242. https://doi.org/10.1007/s12161-021-02086-1

Bradski, G., & Kaehler, A. (2008). *Learning OpenCV*. Sebastopol: O'Reilly Media.

Brosnan, T., & Sun, D.-W. (2004). Improving quality inspection of food products by computer vision-a review. *Journal of Food Engineering*, *61*(1), 3–16. https://doi.org/10.1016/S0260-8774(03)00183-3

Chaudhary, L., & Yogesh, Y. (2019). A comparative study of fruit defect segmentation techniques. *2019 International Conference on Issues and Challenges in Intelligent Computing Techniques (ICICT)*, 1–4. Ghaziabad, India: IEEE. https://doi.org/10.1109/ICICT46931.2019.8977692

Goñi, S. M., & Salvadori, V. O. (2017). Color measurement: comparison of colorimeter vs. computer vision system. *Journal of Food Measurement and Characterization*, *11*(2), 538–547. https://doi.org/10.1007/s11694-016-9421-1

He, Y., Xiao, Q., Bai, X., Zhou, L., Liu, F., & Zhang, C. (2021). Recent progress of nondestructive techniques for fruits damage inspection: a review. *Critical Reviews in Food Science and Nutrition*, *0*(0), 1–19. https://doi.org/10.1080/10408398.2021.1885342

Hu, M.-K. (1962). Visual pattern recognition by moment invariants. *IEEE Transactions on Information Theory*, *8*(2), 179–187. https://doi.org/10.1109/TIT.1962.1057692

Khanam, Al-Naji, & Chahl. (2019). Remote monitoring of vital signs in diverse non-clinical and clinical scenarios using computer vision systems: A review. *Applied Sciences*, *9*(20), 4474. https://doi.org/10.3390/app9204474

Laabassi, K., Belarbi, M. A., Mahmoudi, S., Mahmoudi, S. A., & Ferhat, K. (2021). Wheat varieties identification based on a deep learning approach. *Journal of the Saudi Society of Agricultural Sciences*, *20*(5), 281–289. https://doi.org/10.1016/j.jssas.2021.02.008

Larose, D. T., & Larose, C. D. (2014). *Discovering Knowledge in Data: An Introduction to Data Mining*. Hoboken, N.J., USA: John Wiley & Sons, Inc.

Li, Y., Feng, X., Liu, Y., & Han, X. (2021). Apple quality identification and classification by image processing based on convolutional neural networks. *Scientific Reports*, *11*(1), 16618. https://doi.org/10.1038/s41598-021-96103-2

Liu, L., Li, Z., Lan, Y., Shi, Y., & Cui, Y. (2019a). Design of a tomato classifier based on machine vision. *PLOS ONE*, *14*(7), e0219803. https://doi.org/10.1371/journal.pone.0219803

Liu, Z., Zhang, Z., Liu, Y., Dezert, J., & Pan, Q. (2019b). A new pattern classification improvement method with local quality matrix based on K-NN. *Knowledge-Based Systems*, *164*, 336–347. https://doi.org/10.1016/j.knosys.2018.11.001

Lutu, P. E. N., & Engelbrecht, A. P. (2006). A comparative study of sample selection methods for classification. *South African Computer Journal*, *6*(36), 69–85. https://doi.org/10.46298/arima.1880

Mathiassen, J. R., Misimi, E., Østvik, S. O., & Aursand, I. G. (2012). Computer vision in the fish industry. In D.-W. (University C. D. Sun (Ed.), *Computer Vision Technology in the Food and Beverage Industries* (pp. 352–378). Cambridge: Elsevier. https://doi.org/10.1533/9780857095770.3.352

Mikolajczyk, A., & Grochowski, M. (2018). Data augmentation for improving deep learning in image classification problem. *2018 International Interdisciplinary PhD Workshop (IIPhDW)*, 117–122. IEEE. https://doi.org/10.1109/IIPHDW.2018.8388338

Mutneja, D. V. (2015). Methods of image edge detection: A review. *Journal of Electrical & Electronic Systems*, *4*(2), 1000150. https://doi.org/10.4172/2332-0796.1000150

Nanni, L., Paci, M., Brahnam, S., & Lumini, A. (2021). Comparison of different image data augmentation

approaches. *Journal of Imaging*, *7*(12), 254. https://doi.org/10.3390/jimaging7120254

Nashat, S., & Abdullah, M. Z. (2016). Quality Evaluation of Bakery Products. In *Computer Vision Technology for Food Quality Evaluation* (pp. 525–589). Elsevier. https://doi.org/10.1016/B978-0-12-802232-0.00021-9

Nixon, M. S., & Aguado, A. S. (2012). Feature Extraction & Image Processing for Computer Vision. In *Feature Extraction and Image Processing for Computer Vision* (4th Editio). London: Elsevier. https://doi.org/10.1016/C2011-0-06935-1

Ouchtati, S., Chergui, A., Mavromatis, S., Aissa, B., Rafik, D., & Sequeira, J. (2019). Novel method for brain tumor classification based on use of image entropy and seven hu's invariant moments. *Traitement Du Signal*, *36*(6), 483–491. https://doi.org/10.18280/ts.360602

Sekehravani, E. A., Babulak, E., & Masoodi, M. (2020). Implementing canny edge detection algorithm for noisy image. *Bulletin of Electrical Engineering and Informatics*, *9*(4), 1404–1410. https://doi.org/10.11591/eei.v9i4.1837

Solomon, C., & Breckon, T. (2011). *Fundamentals of Digital Image Processing: A Practical Approach with Examples in MATLAB*. Chichester: John Wiley & Sons.

Song, J., Gao, S., Zhu, Y., & Ma, C. (2019). A survey of remote sensing image classification based on CNNs. *Big Earth Data*, *3*(3), 232–254. https://doi.org/10.1080/20964471.2019.1657720

Taheri-Garavand, A., Fatahi, S., Omid, M., & Makino, Y. (2019). Meat quality evaluation based on computer vision technique: A review. *Meat Science*, *156*(June), 183–195. https://doi.org/10.1016/j.meatsci.2019.06.002

Teixeira, G. H. de A., Meakem, V., Morais, C. de L. M. de, Lima, K. M. G. de, & Whitehead, S. R. (2020). Conventional and alternative pre-harvest treatments affect the quality of 'Golden delicious' and 'York' apple fruit. *Environmental and Experimental Botany*, *173*(February), 104005. https://doi.org/10.1016/j.envexpbot.2020.104005

Tian, H., Wang, T., Liu, Y., Qiao, X., & Li, Y. (2020). Computer vision technology in agricultural automation —A review. *Information Processing in Agriculture*, *7*(1), 1–19. https://doi.org/10.1016/j.inpa.2019.09.006

Tripathi, M. K., & Maktedar, D. D. (2020). A role of computer vision in fruits and vegetables among various horticulture products of agriculture fields: A survey. *Information Processing in Agriculture*, *7*(2), 183–203. https://doi.org/10.1016/j.inpa.2019.07.003

Uji, T. (2007). Review: Species diversity of indigenous fruits in Indonesia and its potential. *Biodiversitas Journal of Biological Diversity*, *8*(2), 157–167. https://doi.org/10.13057/biodiv/d080217

Witus, I. K., On, C. K., Alfred, R., Ibrahim, A. A. A., Guan, T. T., & Anthony, P. (2018). A review of computer vision methods for fruit recognition. *Advanced Science Letters*, *24*(2), 1538–1542. https://doi.org/10.1166/asl.2018.10786

Xu, Y., & Goodacre, R. (2018). On splitting training and validation set: A comparative study of cross-validation, bootstrap and systematic sampling for estimating the generalization performance of supervised learning. *Journal of Analysis and Testing*, *2*(3), 249–262. https://doi.org/10.1007/s41664-018-0068-2